The Quiescent Counterpart of the Peculiar X-Ray Burster SAX J2224.9+5421

Degenaar, N.; Wijnands, R.; Miller, J.M.

Published in:
Astrophysical Journal

DOI:
10.1088/0004-637X/787/1/67

The Astrophysical Journal, 787:67 (6pp), 2014 May 20 doi:10.1088/0004-637X/787/1/67

THE QUIESCENT COUNTERPART OF THE PECULIAR X-RAY BURSTER SAX J2224.9+5421

N. Degenaar[1,3], R. Wijnands[2], and J. M. Miller[1]
[1] Department of Astronomy, University of Michigan, 500 Church Street, Ann Arbor, MI 48109, USA; degenaar@umich.edu
[2] Astronomical Institute Anton Pannekoek, University of Amsterdam, Postbus 94249, 1090 GE Amsterdam, The Netherlands
Received 2013 December 17; accepted 2014 April 11; published 2014 May 5

ABSTRACT

SAX J2224.9+5421 is an extraordinary neutron star low-mass X-ray binary. It was discovered when it was exhibiting a $\simeq 10$ s long thermonuclear X-ray burst, but it had faded to a 0.5–10 keV luminosity of $L_{\rm X} \lesssim 8 \times 10^{32} (D/7.1\,{\rm kpc})^2\,{\rm erg\,s^{-1}}$ only $\simeq 8$ hr later. It is generally assumed that neutron stars are quiescent (i.e., not accreting) at such intensity, raising questions about the trigger conditions of the X-ray burst and the origin of the faint persistent emission. We report on a $\simeq$51 ks *XMM-Newton* observation aimed at finding clues explaining the unusual behavior of SAX J2224.9+5421. We identify a likely counterpart that is detected at $L_{\rm X} \simeq 5 \times 10^{31} (D/7.1\,{\rm kpc})^2\,{\rm erg\,s^{-1}}$ (0.5–10 keV) and has a soft X-ray spectrum that can be described by a neutron star atmosphere model with a temperature of $kT^{\infty} \simeq 50$ eV. This would suggest that SAX J2224.9+5421 is a transient source that was in quiescence during our *XMM-Newton* observation and experienced a very faint (ceasing) accretion outburst at the time of the X-ray burst detection. We consider one other potential counterpart that is detected at $L_{\rm X} \simeq 5 \times 10^{32} (D/7.1\,{\rm kpc})^2\,{\rm erg\,s^{-1}}$ and displays an X-ray spectrum that is best described by a power law with a photon index of $\Gamma \simeq 1.7$. Similarly hard X-ray spectra are seen for a few quiescent neutron stars and may be indicative of a relatively strong magnetic field or the occurrence of low-level accretion.

Key words: accretion, accretion disks – stars: individual (SAX J2224.9+5421) – stars: neutron – X-rays: binaries

Online-only material: color figures

1. INTRODUCTION

When matter accretes onto the surface of a neutron star, it can undergo unstable thermonuclear burning, resulting in a brief, intense flash of X-ray emission. Such thermonuclear X-ray bursts (type-I X-ray bursts; X-ray bursts hereafter) are observed from low-mass X-ray binaries (LMXBs), in which a neutron star accretes matter from a sub-solar companion star that overflows its Roche lobe. X-ray bursts are a potential tool to constrain the fundamental properties of neutron stars (e.g., van Paradijs 1979; Steiner et al. 2010; Suleimanov et al. 2011) and can give valuable insight into the accretion flow around the compact object (e.g., Yu et al. 1999; Ballantyne & Strohmayer 2004; in 't Zand et al. 2012; Degenaar et al. 2013a; Worpel et al. 2013).

Wide-field monitoring with observatories such as *BeppoSAX*, *Integral*, and *Swift* has led to the discovery of X-ray bursts for which no persistent emission could be detected above the instrument background (e.g., in 't Zand et al. 1999; Cocchi et al. 2001; Cornelisse et al. 2002b; Chelovekov & Grebenev 2007; Del Santo et al. 2007; Wijnands et al. 2009; Linares et al. 2009; Degenaar et al. 2010, 2011, 2013a). This implies that these *burst-only sources* are accreting at 2–10 keV luminosities of $L_{\rm X} \lesssim 10^{36}\,{\rm erg\,s^{-1}}$. This is lower than typically seen for neutron star LMXBs (e.g., Chen et al. 1997; Wijnands et al. 2006; Campana 2009; Degenaar et al. 2012b). The burst-only sources trace a relatively unexplored accretion regime and provide valuable new input for thermonuclear burning models (e.g., Cooper & Narayan 2007; Peng et al. 2007; Degenaar et al. 2010).

Follow-up observations with more sensitive narrow-field instruments (e.g., on board *BeppoSAX*, *Chandra*, *XMM-Newton*, and *Swift*) have revealed that the burst-only sources fall into two categories: (1) LMXBs accreting (quasi-) persistently at $L_{\rm X} \simeq 10^{34-35}\,{\rm erg\,s^{-1}}$ (e.g., in 't Zand et al. 2005; Chelovekov & Grebenev 2007; Del Santo et al. 2007; Degenaar et al. 2010), and (2) transient LMXBs that exhibit weeks- to months-long outbursts of $L_{\rm X} \simeq 10^{34-36}\,{\rm erg\,s^{-1}}$, but are otherwise quiescent (e.g., Cocchi et al. 2001; Cornelisse et al. 2002b; Hands et al. 2004; Wijnands et al. 2009; Campana 2009).

In quiescence, neutron star LMXBs are dim with $L_{\rm X} \simeq 10^{31-33}\,{\rm erg\,s^{-1}}$ (e.g., Campana et al. 1998; Jonker et al. 2004; Heinke et al. 2009; Guillot et al. 2013). The quiescent spectra typically contain a soft component that is well-fitted by a neutron star atmosphere model. This emission is ascribed to thermal radiation from the surface of the neutron star, and may act as a probe of its interior properties (e.g., van Paradijs & Verbunt 1984; Brown et al. 1998; Rutledge et al. 1999; Wijnands et al. 2004; Cackett et al. 2006; Degenaar et al. 2013b). With their low mass-accretion rates, the burst-only sources can provide valuable new insight into the thermal evolution of neutron stars (Wijnands et al. 2013).

An additional, non-thermal spectral component is often present in the quiescent spectra. It can be described by a simple power law with a photon index of $\Gamma \simeq 1$–2. This component has been associated with (stochastic) intensity variations and therefore tentatively ascribed to the presence of a residual accretion flow (e.g., Rutledge et al. 2002; Cackett et al. 2005, 2011; Fridriksson et al. 2011; Degenaar & Wijnands 2012; Bernardini et al. 2013; Wijnands & Degenaar 2013). Since there are some indications that the hard power-law emission is particularly prominent in the quiescent spectra of accreting millisecond X-ray pulsars (AMXPs; e.g., Wijnands et al. 2005b; Campana et al. 2008; Heinke et al. 2009; Degenaar et al. 2012a; Linares et al. 2014), it has also been explained as the result of accretion onto the magnetosphere of the neutron star, or a shock from a pulsar wind colliding with matter flowing out of the donor star (e.g., Campana et al. 1998; Rutledge et al. 2001; Linares et al. 2014).

[3] Hubble Fellow.

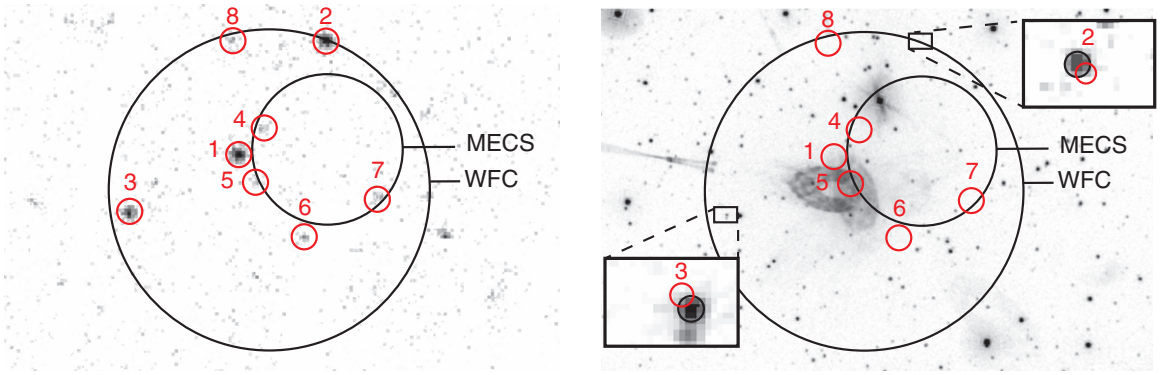

Figure 1. *XMM-Newton* images of the field around J2224. Left: combined EPIC X-ray image (0.5–10 keV). The *BeppoSAX*/WFC positional uncertainty of the X-ray burst (3′.2) and that of the tentative counterpart identified in follow-up *BeppoSAX*/MECS observations (1′.5) are indicated. Within the WFC error circle there were eight faint X-ray sources detected with all three EPIC detectors, which are indicated by numbered red circles (15″ in size). Right: OM *V*-band image. The insets show magnifications to indicate possible associations with optical objects (black circles). In those sub-images the size of the red circles corresponds to the X-ray positional uncertainties of sources 2 and 3 (1″.7 and 1″.6, respectively). The ellipsoidal feature in the center of the image concerns an artifact (stray light).
(A color version of this figure is available in the online journal.)

Table 1
Positions and Basic Properties of Detected X-Ray Sources

Source	R.A. (J2000)	Decl. (J2000)	Error (″)	MOS Count Rate (10^{-3} counts s^{-1})	PN Count Rate (10^{-2} counts s^{-1})	PN Hardness Ratio
1	22 24 52.94	+54 22 38.2	1.6	3.9 ± 0.3	1.3 ± 0.1	0.94 ± 0.17
2	22 25 07.87	+54 21 30.2	1.7	3.2 ± 0.3	0.8 ± 0.1	0.73 ± 0.15
3	22 24 40.99	+54 24 54.4	1.6	3.8 ± 0.3	1.5 ± 0.1	$0.06^{+0.37}_{-0.06}$
4	22 24 49.65	+54 23 10.1	2.3	0.7 ± 0.2	0.17 ± 0.03	$0.22^{+0.58}_{-0.22}$
5	22 24 50.64	+54 22 05.1	2.4	0.6 ± 0.2	0.13 ± 0.03	1.22 ± 0.46
6	22 24 43.99	+54 20 59.9	2.2	0.6 ± 0.2	0.23 ± 0.05	1.54 ± 0.52
7	22 24 33.82	+54 21 48.9	2.2	0.7 ± 0.2	0.24 ± 0.04	1.99 ± 0.34
8	22 24 53.74	+54 24 54.9	2.1	0.6 ± 0.2	0.23 ± 0.04	2.29 ± 0.32

Notes. The quoted positional uncertainties are at 90% confidence level, and are a combination of the statistical error from the detection algorithm and an estimated systematic uncertainty of 1″.5 (Watson et al. 2009). Count rates errors are at the 1σ level of confidence. We consider sources 1 and 4 as possible counterparts for J2224.

1.1. The Peculiar X-Ray Burster SAX J2224.9+5421

Perhaps the most tantalizing burst-only source is SAX J2224.9+5421 (J2224 hereafter). It was detected with the *BeppoSAX* Wide-Field Camera (WFC) as a $\simeq$10 s long X-ray flash on 1999 November 6 (Gandolfi 1999). Initially dubbed GRB 991106, multi-wavelength follow-up observations failed to detect a fading afterglow and cast doubt on a gamma-ray burst (GRB) nature (e.g., Antonelli et al. 1999; Gandolfi et al. 1999; Frail 1999; Jensen et al. 1999; Gorosabel et al. 1999). Cornelisse et al. (2002b) demonstrated that the properties of the event were consistent with a thermonuclear X-ray burst, which would identify J2224 as a new neutron star LMXB. A source distance of $D \lesssim 7.1$ kpc was inferred by assuming that the X-ray burst peak did not exceed the Eddington limit ($L_{\rm edd} = 2 \times 10^{38}$ erg s^{-1}).

No accretion emission could be detected with the WFC around the time of the X-ray burst, implying a 2–28 keV luminosity of $L_{\rm X} \lesssim 2 \times 10^{36} (D/7.1\,{\rm kpc})^2$ erg s^{-1} (Cornelisse et al. 2002b). Rapid follow-up observations with the *BeppoSAX* Medium-Energy Concentrator Spectrometer (MECS), performed $\simeq$8 hr after the X-ray burst detection, revealed only one source within the WFC error circle that was detected at a 0.5–10 keV luminosity of $L_{\rm X} \simeq 8 \times 10^{32} (D/7.1\,{\rm kpc})^2$ erg s^{-1} (Antonelli et al. 1999). This raises the question whether the X-ray burst was ignited when the neutron star was accreting at a very low level, or whether it exhibited a faint, undetected accretion outburst that had ceased within 8 hr of the X-ray burst detection.

In this work, we present a deep *XMM-Newton* observation to search for an X-ray counterpart of J2224, and to find clues to its nature and unusual behavior.

2. OBSERVATIONS AND ANALYSIS

2.1. X-Ray Data

The field around J2224 was observed with *XMM-Newton* for $\simeq$51 ks on 2013 May 29 UT 06:04–20:24 (ID 0720880101). X-ray data was obtained with the European Photon Imaging Camera (EPIC), which consists of two Metal Oxide Semiconductor (MOS) detectors (Turner et al. 2001) and one PN camera (Strüder et al. 2001). All instruments were operated in the full frame imaging mode with the medium optical blocking filter applied. We reduced and analyzed the data using the Science Analysis software (version 11.0). The original data files were reprocessed using the tasks EMPROC and EPPROC. The observation was free from background flaring.

Figure 1 (left) displays the composite X-ray image of all three detectors. There are eight faint X-ray sources within the *BeppoSAX*/WFC error circle that were detected with all three EPIC instruments. The source positions (determined using the task EDETECT_CHAIN) are listed in Table 1. Sources 1 and 3 were previously detected at similar intensities in *Swift*/XRT data of the field (named SAX J2225-1 and SAX J2225-2, respectively; Campana 2009).

We determined the count rate for each source by employing the task EREGIONANALYSE, using circular regions with radius of 20″ (400 pixels) centered on the source positions. For the background we used a circular region with a radius of 60″ placed on a source-free part of the CCD. Source and background spectra were extracted using ESPECGET, which also generated the response files. We co-added the two MOS spectra and their response files with EPICSPECCOMBINE. Using GRPPHA, the spectral data was grouped to contain a minimum of 15 photons per bin. We used XSPEC (version 12.7; Arnaud 1996) to perform spectral fits in an energy range of 0.5–10 keV.

2.2. X-Ray Spectral Analysis

To obtain a rough characterization of the spectral shape, we determined the hardness ratio for each source using the PN data. For the present purpose, we defined this quantity as the ratio of counts in the 2–10 and 0.5–2 keV bands. This information is included in Table 1.

We explored their X-ray spectra using two models that are widely used for neutron star LMXBs at low luminosities: a simple power law (PEGPWRLW in XSPEC) and a neutron star atmosphere model (for which we chose NSATMOS; Heinke et al. 2006). For the latter we always fixed the neutron star mass ($M = 1.4\,M_{\odot}$) and radius ($R = 10$ km) as well as the distance ($D = 7.1$ kpc) and the normalization (unity). The neutron star temperature was then the only free fit parameter. Thermal bolometric fluxes were estimated by extrapolating the NSATMOS model fits to the 0.01–100 keV energy range. In all spectral fits, we accounted for interstellar absorption by including the TBABS model in XSPEC, using the WILM abundances and VERN cross-sections (Verner et al. 1996; Wilms et al. 2000).

2.3. Optical and Ultraviolet Data

Quasi-simultaneous optical and ultraviolet (UV) coverage was provided by the Optical Monitor (OM; Mason et al. 1996). The position of J2224 was observed with the OM operated in image mode. Exposures of 2000, 2460, and 2200 s were obtained using the V ($\lambda_c \simeq 5407$ Å), $UVW1$ ($\lambda_c \simeq 2905$ Å), and $UVW2$ ($\lambda_c \simeq 2070$ Å) filters, respectively. Reduction, source detection, and photometry were performed using the meta-task OMICHAIN.

None of the X-ray sources within the *BeppoSAX* uncertainty of J2224 are detected in the $UVW2$ image. However, sources 2 and 3 both have a potential counterpart in the V and $UVW1$ wavebands. This is illustrated in Figure 1 (right), which shows the OM V-band image.

3. RESULTS

3.1. Sources 5–8: Too X-Ray Hard

Sources 5–8 have the hardest spectra among the detected sources, as indicated by their high hardness ratios (Table 1). Although a limited number of counts prohibits a detailed analysis, their spectra can be described by a power law with photon indices of $\Gamma \simeq 1$–3 and hydrogen column densities that are well in excess of the Galactic value in the direction of J2224 ($N_{\rm H} \simeq 4.6 \times 10^{21}$ cm^{-2}; Kalberla et al. 2005). This renders them unlikely counterparts to the X-ray burster. Their unabsorbed fluxes lie in the range of $F_{\rm X,unabs} \simeq (1\text{–}10) \times 10^{-14}$ erg cm^{-2} s^{-1} (0.5–10 keV).

It is more likely that these hard X-ray sources are (obscured) background active galactic nuclei (AGNs) or Galactic accreting white dwarfs (i.e., cataclysmic variables (CVs); see also Section 3.2). Both types of objects are abundant in the sky. For example, assuming a number density of $\simeq 3 \times 10^{-5}$ pc^{-3} (e.g., Schwope et al. 2002), we expect $\simeq 3$ CVs within the WFC error circle. Furthermore, down to a flux of $\simeq 10^{-14}$ erg cm^{-2} s^{-1}, about 3×10^2 AGNs are expected per square degree of sky (Brandt & Hasinger 2005). That implies that within the WFC uncertainty, roughly three AGNs with fluxes of $\gtrsim 10^{-14}$ erg cm^{-2} s^{-1} are expected.

3.2. Sources 2 and 3: Too Optically/UV Bright

Sources 2 and 3 are the only ones with possible optical/UV associations. Based on the total number of V-band objects detected within the $17' \times 17'$ OM field of view, we estimate the probability of a chance alignment within the 1.″6 and 1.″7 positional uncertainties of sources 2 and 3 to be $\simeq 5 \times 10^{-3}$ and $\simeq 6 \times 10^{-3}$, respectively.

For source 2 we measure AB magnitudes of $V = 16.41 \pm 0.01$ mag and $UVW1 = 17.45 \pm 0.05$ mag. The corresponding flux densities are $f_V = (1.1 \pm 0.1) \times 10^{-15}$ erg cm^{-2} s^{-1} Å^{-1} and $f_{UVW1} = (3.8 \pm 0.2) \times 10^{-16}$ erg cm^{-2} s^{-1} Å^{-1} (uncorrected for reddening). The X-ray spectrum of source 2 cannot be described by a neutron star atmosphere model ($\chi^2_\nu > 3$), but fits a power law with $\Gamma = 2.0 \pm 0.3$ and $N_{\rm H} \simeq (6.9 \pm 2.3) \times 10^{21}$ cm^{-2}. The resulting 0.5–10 keV unabsorbed flux is $F_{\rm X,unabs} \simeq (4.9 \pm 0.7) \times 10^{-14}$ erg cm^{-2} s^{-1}.

By multiplying the obtained V flux density with the width of the filter ($\simeq 684$ Å), we obtain a ratio of the X-ray to optical flux of $F_{\rm X}/F_V \simeq 0.3$ for source 2. Quiescent neutron star LMXBs typically have a much higher X-ray flux compared to that in the optical/UV band (a ratio of $\simeq 10$ or higher; e.g., Homer et al. 2001; Russell et al. 2006; Hynes & Robinson 2012). We therefore consider it unlikely that source 2 is the counterpart to J2224. It is plausible that it is a background AGN (see also Section 3.1). The X-ray spectra of these objects can typically be described by a $\Gamma \simeq 2$ power-law model, and their X-ray/optical flux ratios fall in a wide range of $F_{\rm X}/F_V \simeq 0.1$–10.

Source 3, for which we measure $V = 18.08 \pm 0.07$ mag ($f_V = (2.3 \pm 0.2) \times 10^{-16}$ erg cm^{-2} s^{-1} Å^{-1}) and $UVW1 = 19.10 \pm 0.19$ mag ($f_{UVW1} = (8.4 \pm 1.4) \times 10^{-17}$ erg cm^{-2} s^{-1} Å^{-1}), also seems too optically/UV bright for a quiescent neutron star LMXB. This is supported by the fact that neither a power law nor a neutron star atmosphere model, or a combination of the two, can satisfactory describe the X-ray spectrum of source 3 (all trials resulted in $\chi^2_\nu > 1.5$ for 53–55 degrees of freedom (dof)). The data is instead better fitted with, e.g., a combination of a blackbody and an optically thin thermal plasma model (MEKAL; yielding $\chi^2_\nu = 1.07$ for 52 dof), or a double MEKAL model ($\chi^2_\nu = 1.14$ for 52 dof). Such models are often used to describe the spectra of (magnetic) CVs (e.g., Ramsay et al. 2004; Baskill et al. 2005). Indeed, we expect several CVs are present within the WFC error circle of J2224 (see Section 3.1).

3.3. Source 4: An X-Ray Soft Candidate Counterpart

Source 4 stands out by showing a relatively soft X-ray spectrum that can be described by an absorbed power-law model with $\Gamma = 2.9^{+2.2}_{-1.0}$ and $N_{\rm H} = 2.8^{+4.5}_{-2.2} \times 10^{21}$ cm^{-2} (Table 2). The obtained hydrogen column density is consistent with the Galactic value in the direction of J2224. A neutron star atmosphere model provides a good fit, yielding a neutron star temperature (as seen by an observer at infinity) of $kT^{\infty} = 50 \pm 4$ eV and $N_{\rm H} = (4.8 \pm 0.2) \times 10^{21}$ cm^{-2}. The obtained 0.5–10 keV luminosity is $L_{\rm X} \simeq 5 \times 10^{31} (D/7.1\,{\rm kpc})^2$ erg s^{-1}. The X-ray

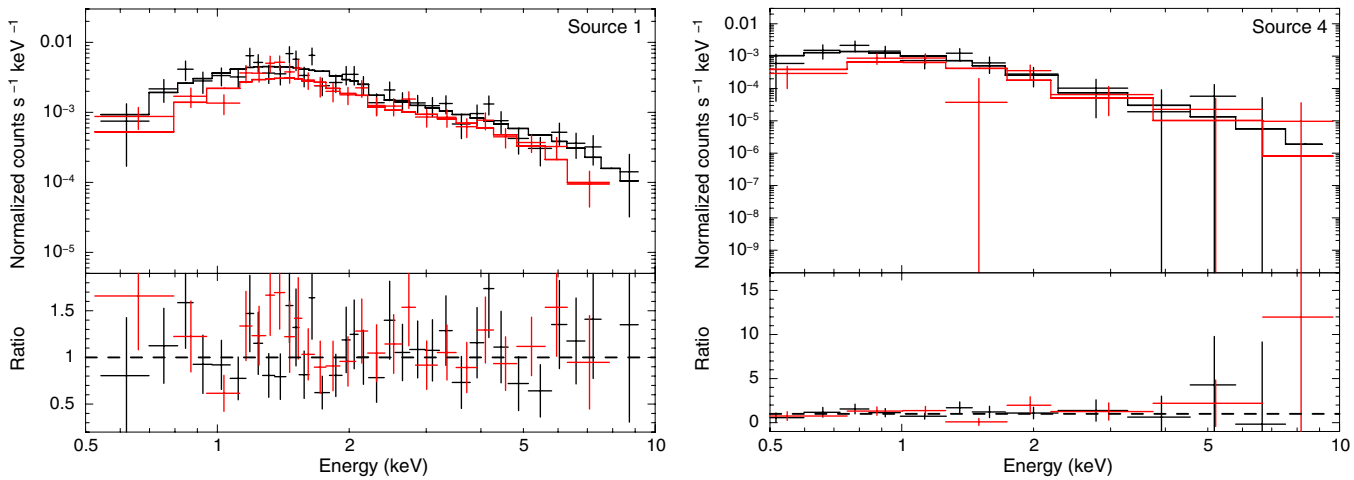

Figure 2. *XMM-Newton* PN (black) and combined MOS1/MOS2 (red) spectra of the two candidate counterparts of J2224. The solid lines indicate the model fits: a power law for source 1 and a neutron star atmosphere model for source 4 (see Section 3). The bottom panels show the model-to-data ratio.
(A color version of this figure is available in the online journal.)

Table 2
Spectral Results of the Two Candidate X-Ray Counterparts

	Source 1		Source 4	
Parameter (Unit)/Model	POW	POW+NSATMOS	POW	NSATMOS
$N_{\rm H}$ ($\times 10^{21}$ cm^{-2})	6.7 ± 1.9	7.0 ± 2.7	$2.8^{+4.5}_{-2.2}$	4.8 ± 0.2
Γ	1.7 ± 0.2	1.7 ± 0.2	$2.9^{+2.2}_{-1.0}$	
kT^{∞} (eV)		<61		50 ± 4
χ^2/dof	52.4/58	52.3/57	10.9/16	16.0/17
$F_{\rm X,abs}$ ($\times 10^{-14}$ erg cm^{-2} s^{-1})	6.0 ± 0.5	6.0 ± 0.6	0.4 ± 0.2	0.2 ± 0.1
$F_{\rm X,unabs}$ ($\times 10^{-14}$ erg cm^{-2} s^{-1})	7.8 ± 0.8	8.0 ± 1.5	$0.6^{+1.8}_{-0.1}$	0.9 ± 0.4
$L_{\rm X}$ ($\times 10^{32}(D/7.1\,{\rm kpc})^2$ erg s^{-1})	4.7 ± 0.5	4.8 ± 0.7	$0.4^{+1.0}_{-0.1}$	0.5 ± 0.2
$L_{\rm th}$ ($\times 10^{32}(D/7.1\,{\rm kpc})^2$ erg s^{-1})		<3.1		1.4 ± 0.5
Thermal contribution		$<24\%$		

Notes. Quoted errors represent 90% confidence levels. $F_{\rm X,abs}$ and $F_{\rm X,unabs}$ represent the 0.5–10 keV absorbed and unabsorbed flux, respectively. $L_{\rm X}$ denotes the 0.5–10 keV luminosity and $L_{\rm th}$ the 0.01–100 keV thermal luminosity. The bottom row gives the contribution of the thermal NSATMOS component to the total unabsorbed 0.5–10 keV model flux.

spectrum of source 4 is shown in Figure 2 (right), and the fit results are summarized in Table 2.

The spectral shape of source 4 is typical for a quiescent neutron star LMXB. Combined with its location near the center of the *BeppoSAX*/WFC error circle, and lack of an optical/UV association, source 4 is a strong candidate counterpart to J2224. The intensity inferred from our *XMM-Newton* observation is well below the sensitivity of previous X-ray observations that covered the source region (e.g., with *BeppoSAX* and *Swift*; Antonelli et al. 1999; Campana 2009), which explains why this object was not found before.

3.4. Source 1: An X-Ray-hard Candidate Counterpart

A neutron star atmosphere model fails to describe the spectral data of source 1 ($\chi^2_\nu > 3$). However, a power law provides an adequate fit, yielding $\Gamma = 1.7 \pm 0.2$ and $N_{\rm H} \simeq (6.7 \pm 1.9) \times 10^{21}$ cm^{-2} (comparable to the Galactic value toward J2224). The inferred 0.5–10 keV luminosity is $L_{\rm X} \simeq 5 \times 10^{32}(D/7.1\,{\rm kpc})^2$ erg s^{-1}. The X-ray spectrum of source 1 is shown in Figure 2 (left).

Although the spectral shape of source 1 is harder than that typically observed for quiescent neutron star LMXBs, there are a few sources with similar properties (see Section 4). Combined with its location near the center of the *BeppoSAX*/WFC error circle and lack of a bright optical/UV association, we cannot discard source 1 as a potential counterpart. This object was detected during *Swift*/XRT observations obtained in 2006–2008 at $L_{\rm X} \simeq 8 \times 10^{32}(D/7.1\,{\rm kpc})^2$ erg s^{-1} (Campana 2009), i.e., similar as during our *XMM-Newton* observation.

We probed the upper limits on any thermal emission by adding an NSATMOS component to the best power-law fit. This yielded $kT^{\infty} \lesssim 61$ eV and a fractional contribution of the thermal component to the total unabsorbed 0.5–10 keV model flux of $\lesssim$24%. The spectral results of source 1 are listed in Table 2.

4. DISCUSSION

4.1. The Counterpart to the X-Ray Burst

J2224 is one of several sources for which *BeppoSAX* detected an X-ray flash without detectable accretion emission (e.g., Cornelisse et al. 2002b). Follow-up observations were performed with *Chandra* for some of these objects (several years later) and revealed weak candidate X-ray counterparts with $L_{\rm X} \lesssim 5 \times 10^{32}$ erg s^{-1}. This suggested that they were likely transient neutron star LMXBs that exhibited faint ($L_{\rm X} \lesssim 10^{36}$ erg s^{-1}) accretion outbursts when the X-ray

bursts were ignited (Cornelisse et al. 2002a). Indeed, several of these sources were later detected during faint accretion outbursts (e.g., SAXJ1828.5–1037, SAXJ1753.5–2349, and SAXJ1806.5–2215; Hands et al. 2004; Degenaar & Wijnands 2008; Del Santo et al. 2010; Altamirano et al. 2011b).

The quality of the WFC data of J2224 was very low, imposing considerable uncertainty on the interpretation of this event (Cornelisse et al. 2002b). However, the similarities between the X-ray flash from J2224 and that of the other sources (i.e., duration, peak flux, overall spectral properties, indication of softening during the decay, and location in the Galactic plane) renders it likely that J2224 too is a bursting neutron star (Cornelisse et al. 2002b). Here we identify two possible quiescent neutron star LMXBs within the WFC error circle that provide support for this interpretation.

During our long *XMM-Newton* observation, we detected eight weak X-ray sources within the 3.′2 *BeppoSAX*/WFC uncertainty of J2224. They had 0.5–10 keV luminosities in the range of $L_{\rm X} \simeq (0.5\text{–}5) \times 10^{32} (D/7.1\,{\rm kpc})^2\,{\rm erg\,s^{-1}}$, which is typical for transient neutron star LMXBs in quiescence (see, e.g., Jonker et al. 2004). However, based on the X-ray spectral properties and X-ray/optical luminosity ratios, we can discard six of these as potential counterparts to the X-ray burster, leaving only sources 1 and 4 as candidates.

Source 1 was detected at $L_{\rm X} \simeq 5 \times 10^{32} (D/7.1\,{\rm kpc})^2\,{\rm erg\,s^{-1}}$, with a spectrum best described by a power-law model with an index of $\Gamma = 1.7$. Emission from a neutron star atmosphere with $kT^{\infty} \lesssim 61$ eV could contribute up to $\simeq$24% to the total unabsorbed 0.5–10 keV flux. Only a handful of quiescent neutron star LMXBs have similarly hard X-ray spectra that lack detectable thermal emission. The small LMXB subclass of AMXPs (which display coherent X-ray pulsations during accretion outbursts) exhibit $\Gamma \simeq 1.5$ power-law spectra with $\lesssim$40% attributed to thermal emission (e.g., SAX J1808.4–3658, Swift J1749.4–2807, and IGR J18245–2452; Campana et al. 2008; Heinke et al. 2009; Degenaar et al. 2012a; Linares et al. 2014). Their hard spectra are ascribed to their relatively strong magnetic field. The only non-pulsating neutron star with a very hard ($\Gamma \simeq 1.7$) quiescent spectrum is the LMXB and X-ray burster EXO 1745–248 (e.g., Wijnands et al. 2005a; Degenaar & Wijnands 2012). Its irregular quiescent properties have been interpreted in terms of ongoing low-level accretion. Thus, source 1 could be the counterpart of J2224, but it would imply that it is an unusual neutron star (perhaps with a relatively strong magnetic field or exhibiting low-level accretion).

Source 4, on the other hand, has a soft X-ray spectrum like the majority of quiescent neutron star LMXBs. This source was detected at $L_{\rm X} \simeq 5 \times 10^{31} (D/7.1\,{\rm kpc})^2\,{\rm erg\,s^{-1}}$, and its spectrum can be described by a neutron star atmosphere model with $kT^{\infty} \simeq 50$ eV. This relatively low temperature is consistent with the expectations for a neutron star that exhibits faint accretion outbursts (Wijnands et al. 2013). We therefore tentatively identify source 4 as the counterpart of the X-ray burst detected with *BeppoSAX* in 1999.

4.2. The X-Ray Burst Trigger Conditions

The duration, repetition rate, and energetics of X-ray bursts depend on the conditions of the ignition layer, such as its thickness, temperature profile, and chemical abundances. These conditions are sensitive to the (local) accretion rate onto the neutron star so that different accretion regimes give rise to X-ray bursts with distinct properties (e.g., Fujimoto et al. 1981; Fushiki & Lamb 1987). X-ray bursts that ignite in a pure He layer are typically short (seconds), whereas the presence of H in the ignition layer prolongs the duration (minutes).

Upper limits obtained for the accretion emission of the burst-only sources suggests they occupy the lowest accretion regime ($\lesssim$0.01 $L_{\rm Edd}$; Cornelisse et al. 2002b). Classical burning theory prescribes that in this regime unstable burning of H should trigger a mixed He/H X-ray burst with a duration of $\simeq$100 s (e.g., Fujimoto et al. 1981). This is much longer than the short ($\simeq$10 s) X-ray bursts detected from J2224 and other *BeppoSAX* burst-only sources. This apparent discrepancy was addressed by Peng et al. (2007), who showed that for the low inferred mass-accretion rates, sedimentation of heavy elements significantly reduces the amount of H in the ignition layer. This would alter the X-ray burst properties, possibly accounting for the observed short duration of the X-ray bursts (Peng et al. 2007).

The fact that no persistent X-ray emission was detected above $L_{\rm X} \simeq 8 \times 10^{32} (D/7.1\,{\rm kpc})^2\,{\rm erg\,s^{-1}}$ within $\simeq$8 hr after the X-ray burst detection raises the question whether J2224 may have been accreting at $\lesssim 1 \times 10^{-5}\,L_{\rm Edd}$ when the burst ignited. This is right at the boundary below which theoretical models predict that no X-ray bursts can occur (e.g., Fushiki & Lamb 1987). We consider this scenario unlikely, because the chance probability of detecting this $\simeq$10 s event would be very low; for a typical ignition column depth of $y \simeq 10^8\,{\rm g\,cm^{-2}}$ and a mass-accretion rate of $\dot{M} \simeq 10^{-13}\,M_{\odot}\,{\rm yr^{-1}}$, the time to accumulate enough material to produce this X-ray burst would be $\simeq$8 yr.

Regardless whether source 1 or source 4 is the true counterpart, we consider it more likely that J2224 is a transient neutron star LMXB that exhibited an X-ray burst during the decay of a (short) faint accretion outburst. In particular, the behavior of J2224 is strikingly similar to that of the AMXP Swift J1749.4–2807. This source rapidly decayed to a level of $L_{\rm X} \simeq 1 \times 10^{33}\,{\rm erg\,s^{-1}}$ within a day after it was discovered through the detection of an X-ray burst (Wijnands et al. 2009). Its behavior remained a puzzle until it exhibited a $\simeq$2 week long accretion outburst with an average 0.5–10 keV luminosity of $L_{\rm X} \simeq 10^{36}\,{\rm erg\,s^{-1}}$ several years later (e.g., Altamirano et al. 2011a). This suggests that the peculiar X-ray burst had likely occurred during the decay of its previous accretion outburst. A similar scenario can be envisioned for SAX J2224.9+5421.

N.D. is supported by NASA through Hubble Postdoctoral Fellowship grant number HST-HF-51287.01-A from the Space Telescope Science Institute, which is operated by the Association of Universities for Research in Astronomy, Incorporated, under NASA contract NAS5-26555. R.W. acknowledges support from a European Research Council (ERC) starting grant. Support for this work was provided by an *XMM-Newton* GO grant for proposal number 072088. The authors thank the anonymous referee for thoughtful comments that helped improve the clarity of this manuscript.

Facility: XMM (EPIC,OM)

REFERENCES

Altamirano, D., Cavecchi, Y., Patruno, A., et al. 2011a, ApJL, 727, L18
Altamirano, D., Kaur, R., Degenaar, N., et al. 2011b, ATel, 3193
Antonelli, L. A., Gandolfi, G., Feroci, M., et al. 1999, GCN, 445, 1
Arnaud, K. A. 1996, in ASP Conf. Ser. 101, Astronomical Data Analysis Software and Systems V, ed. G. H. Jacoby & J. Barnes (San Francisco, CA: ASP), 17
Ballantyne, D. R., & Strohmayer, T. E. 2004, ApJL, 602, L105
Baskill, D. S., Wheatley, P. J., & Osborne, J. P. 2005, MNRAS, 357, 626
Bernardini, F., Cackett, E. M., Brown, E. F., et al. 2013, MNRAS, 436, 2465
Brandt, W. N., & Hasinger, G. 2005, ARA&A, 43, 827

Brown, E. F., Bildsten, L., & Rutledge, R. E. 1998, ApJL, 504, L95
Cackett, E. M., Fridriksson, J. K., Homan, J., Miller, J. M., & Wijnands, R. 2011, MNRAS, 414, 3006
Cackett, E. M., Wijnands, R., Heinke, C. O., et al. 2005, ApJ, 620, 922
Cackett, E. M., Wijnands, R., Linares, M., et al. 2006, MNRAS, 372, 479
Campana, S. 2009, ApJ, 699, 1144
Campana, S., Colpi, M., Mereghetti, S., Stella, L., & Tavani, M. 1998, A&ARv, 8, 279
Campana, S., Stella, L., Israel, G., & D'Avanzo, P. 2008, ApJL, 689, L129
Chelovekov, I. V., & Grebenev, S. A. 2007, AstL, 33, 807
Chen, W., Shrader, C. R., & Livio, M. 1997, ApJ, 491, 312
Cocchi, M., Bazzano, A., Natalucci, L., et al. 2001, A&A, 378, L37
Cooper, R. L., & Narayan, R. 2007, ApJ, 661, 468
Cornelisse, R., Verbunt, F., in 't Zand, J. J. M., Kuulkers, E., & Heise, J. 2002a, A&A, 392, 931
Cornelisse, R., Verbunt, F., in 't Zand, J. J. M., et al. 2002b, A&A, 392, 885
Degenaar, N., Jonker, P. G., Torres, M. A. P., et al. 2010, MNRAS, 404, 1591
Degenaar, N., Miller, J. M., Wijnands, R., Altamirano, D., & Fabian, A. C. 2013a, ApJL, 767, L37
Degenaar, N., Patruno, A., & Wijnands, R. 2012a, ApJ, 756, 148
Degenaar, N., & Wijnands, R. 2008, ATel, 1831
Degenaar, N., & Wijnands, R. 2012, MNRAS, 422, 581
Degenaar, N., Wijnands, R., Brown, E. F., et al. 2013b, ApJ, 775, 48
Degenaar, N., Wijnands, R., Cackett, E. M., et al. 2012b, A&A, 545, A49
Degenaar, N., Wijnands, R., & Kaur, R. 2011, MNRAS, 414, L104
Del Santo, M., Sidoli, L., Mereghetti, S., et al. 2007, A&A, 468, L17
Del Santo, M., Sidoli, L., Romano, P., et al. 2010, MNRAS, 403, L89
Frail, D. A. 1999, GCN, 444, 1
Fridriksson, J. K., Homan, J., Wijnands, R., et al. 2011, ApJ, 736, 162
Fujimoto, M. Y., Hanawa, T., & Miyaji, S. 1981, ApJ, 247, 267
Fushiki, I., & Lamb, D. Q. 1987, ApJL, 323, L55
Gandolfi, G. 1999, GCN, 434, 1
Gandolfi, G., Soffitta, P., Heise, J., et al. 1999, GCN, 448, 1
Gorosabel, J., Rol, E., Vreeswijk, P., et al. 1999, GCN, 447, 1
Guillot, S., Servillat, M., Webb, N. A., & Rutledge, R. E. 2013, ApJ, 772, 7
Hands, A. D. P., Warwick, R. S., Watson, M. G., & Helfand, D. J. 2004, MNRAS, 351, 31
Heinke, C. O., Jonker, P. G., Wijnands, R., Deloye, C. J., & Taam, R. E. 2009, ApJ, 691, 1035
Heinke, C. O., Rybicki, G. B., Narayan, R., & Grindlay, J. E. 2006, ApJ, 644, 1090
Homer, L., Charles, P. A., Chakrabarty, D., & van Zyl, L. 2001, MNRAS, 325, 1471
Hynes, R. I., & Robinson, E. L. 2012, ApJ, 749, 3
in 't Zand, J. J. M., Cornelisse, R., & Méndez, M. 2005, A&A, 440, 287
in 't Zand, J. J. M., Heise, J., Muller, J. M., et al. 1999, NuPhS, 69, 228
in 't Zand, J. J. M., Homan, J., Keek, L., & Palmer, D. M. 2012, A&A, 547, A47
Jensen, B. L., Pedersen, H., Hjorth, J., Larsen, S., & Costa, E. 1999, GCN, 440, 1
Jonker, P. G., Galloway, D. K., McClintock, J. E., et al. 2004, MNRAS, 354, 666
Kalberla, P. M. W., Burton, W. B., Hartmann, D., et al. 2005, A&A, 440, 775
Linares, M., Bahramian, A., Heinke, C., et al. 2014, MNRAS, 438, 251
Linares, M., Watts, A. L., Wijnands, R., et al. 2009, MNRAS, 392, L11
Mason, K. O., Cropper, M. S., Hunt, R., et al. 1996, Proc. SPIE, 2808, 438
Peng, F., Brown, E. F., & Truran, J. W. 2007, ApJ, 654, 1022
Ramsay, G., Cropper, M., Wu, K., et al. 2004, MNRAS, 350, 1373
Russell, D. M., Fender, R. P., Hynes, R. I., et al. 2006, MNRAS, 371, 1334
Rutledge, R. E., Bildsten, L., Brown, E. F., Pavlov, G. G., & Zavlin, V. E. 1999, ApJ, 514, 945
Rutledge, R. E., Bildsten, L., Brown, E. F., Pavlov, G. G., & Zavlin, V. E. 2001, ApJ, 559, 1054
Rutledge, R. E., Bildsten, L., Brown, E. F., Pavlov, G. G., & Zavlin, V. E. 2002, ApJ, 577, 346
Schwope, A. D., Brunner, H., Buckley, D., et al. 2002, A&A, 396, 895
Steiner, A. W., Lattimer, J. M., & Brown, E. F. 2010, ApJ, 722, 33
Strüder, L., Briel, U., Dennerl, K., et al. 2001, A&A, 365, L18
Suleimanov, V., Poutanen, J., Revnivtsev, M., & Werner, K. 2011, ApJ, 742, 122
Turner, M. J. L., Abbey, A., Arnaud, M., et al. 2001, A&A, 365, L27
van Paradijs, J. 1979, ApJ, 234, 609
van Paradijs, J., & Verbunt, F. 1984, in AIP Conf. Proc. 115, High Energy Transients in Astrophysics, ed. S. E. Woosley (Melville, NY: AIP), 49
Verner, D. A., Ferland, G. J., Korista, K. T., & Yakovlev, D. G. 1996, ApJ, 465, 487
Watson, M. G., Schröder, A. C., Fyfe, D., et al. 2009, A&A, 493, 339
Wijnands, R., & Degenaar, N. 2013, MNRAS, 434, 1599
Wijnands, R., Degenaar, N., & Page, D. 2013, MNRAS, 432, 2366
Wijnands, R., Heinke, C. O., Pooley, D., et al. 2005a, ApJ, 618, 883
Wijnands, R., Homan, J., Heinke, C. O., Miller, J. M., & Lewin, W. H. G. 2005b, ApJ, 619, 492
Wijnands, R., Homan, J., Miller, J. M., & Lewin, W. H. G. 2004, ApJL, 606, L61
Wijnands, R., in 't Zand, J. J. M., Rupen, M., et al. 2006, A&A, 449, 1117
Wijnands, R., Rol, E., Cackett, E., Starling, R. L. C., & Remillard, R. A. 2009, MNRAS, 393, 126
Wilms, J., Allen, A., & McCray, R. 2000, ApJ, 542, 914
Worpel, H., Galloway, D. K., & Price, D. J. 2013, ApJ, 772, 94
Yu, W., Li, T. P., Zhang, W., & Zhang, S. N. 1999, ApJL, 512, L35